CSIRO PUBLISHING

Reproduction, Fertility and Development, 2019, **31**, 1330–1338
https://doi.org/10.1071/RD18276

Vitrifying immature equine oocytes impairs their ability to correctly align the chromosomes on the MII spindle

Kaatje D. Ducheyne[A,B,D], *Marilena Rizzo*[B,C], *Peter F. Daels*[A], *Tom A. E. Stout*[B] *and Marta de Ruijter-Villani*[B]

[A]Department of Medical Imaging and Small Animal Orthopaedics, Faculty of Veterinary Medicine, Ghent University, Salisburylaan 133, 9820 Merelbeke, Belgium.
[B]Department of Equine Sciences, Faculty of Veterinary Medicine, Utrecht University, Yalelaan 112, 3684CM Utrecht, Netherlands.
[C]Department of Veterinary Sciences, Messina University, Viale Annunziata, 98168 Messina, Italy.
[D]Corresponding author. Email: k.d.ducheyne@uu.nl

Abstract. Vitrified–warmed immature equine oocytes are able to complete the first meiotic division, but their subsequent developmental competence is compromised. Therefore, the present study investigated the effects of vitrifying immature horse oocytes on the chromosome and spindle configuration after IVM. Cumulus–oocytes complexes (COCs) were collected and divided into two groups based on mare age (young ≤14 years; old ≥16 years). COCs were then either directly matured *in vitro* or vitrified and warmed before IVM. Spindle morphology and chromosome alignment within MII stage oocytes were assessed using immunofluorescent staining, confocal microscopy and three-dimensional image analysis. Vitrification reduced the ability of oocytes to reach MII and resulted in ultrastructural changes to the meiotic spindle, including shortening of its long axis, and an increased incidence of chromosomes failing to align properly at the metaphase plate. We hypothesise that aberrant chromosome alignment is an important contributor to the reduced developmental competence of vitrified equine oocytes. Contrary to expectation, oocytes from young mares were more severely affected than oocytes from older mares; we propose that the reduced effect of vitrification on oocytes from older mares is related to pre-existing compromise of spindle assembly checkpoint control mechanisms in these mares.

Additional keywords: chromosome alignment, cryopreservation, horse, meiotic spindle.

Received 31 July 2018, accepted 6 February 2019, published online 10 April 2019

Introduction

In the past 5 years, *in vitro* embryo production has become increasingly common in sport horse breeding. In particular, the discovery that oocytes can be held overnight (Choi *et al.* 2006) or transported for up to 18 h (Galli *et al.* 2014) after collection without any negative effect on embryo production has allowed oocyte recovery (ovum pick-up (OPU)) to be performed at locations distant to a laboratory with the equipment and experience to perform the subsequent IVM and intracytoplasmic sperm injection (ICSI). Cryopreservation of oocytes would allow transportation over even longer distances, removing the worries associated with delayed transport and allowing for flexible planning in the ICSI laboratory, thereby make *in vitro* embryo production even more accessible. Moreover, when mares die unexpectedly, oocyte cryopreservation would allow the salvage and storage of female germ line material without the requirement to commit immediately to stallion choice.

Because in mares, unlike other species, there is no reliable, commercially available route to ovarian superstimulation (Roser and Meyers-Brown 2012) OPU is generally performed without any hormonal preparation, and the oocytes collected are immature (germinal vesicle (GV)). Because the most common practical application of oocyte cryopreservation would be collection and freezing at a location distant to the ICSI laboratory, it is more desirable to develop techniques for cryopreserving GV than MII equine oocytes.

However, vitrifying equine GV stage oocytes severely compromises subsequent developmental competence; although an acceptable proportion of oocytes do reach MII after vitrification–warming (13–50%; Hochi *et al.* 1996; Hurtt *et al.* 2000; Tharasanit *et al.* 2006; de Leon *et al.* 2012; Curcio *et al.* 2014; Canesin *et al.* 2017, 2018; Ortiz-Escribano *et al.* 2018), the success of blastocyst production after subsequent ICSI is low (0–15%; Tharasanit *et al.* 2006; Canesin *et al.* 2017, 2018; Ortiz-Escribano *et al.* 2018) compared with that achieved after ICSI of non-cryopreserved oocytes (23–39%; Galli *et al.* 2007; Choi *et al.* 2016; Rader *et al.* 2016). In addition, blastocysts produced from vitrified oocytes result in a lower percentage of foals born (1/5: 20%) after transfer to recipient mares (Ortiz-Escribano *et al.* 2018) than blastocysts produced *in vitro* from

non-cryopreserved oocytes (38–52%; Galli *et al.* 2007; Choi *et al.* 2016; Rader *et al.* 2016).

During meiosis, oocytes undergo two rounds of chromosome segregation (meiosis I and meiosis II) to produce a haploid gamete that is able, after fusion with a spermatozoon during fertilisation, to yield a normal diploid zygote and embryo. During oocyte maturation, meiosis I resumes and is completed, with the oocyte then immediately embarking on meiosis II, before arresting again at MII until fertilisation occurs. Formation of the MI and MII spindles and accurate alignment of the chromosome pairs (homologous chromosomes during MI; sister chromatids during MII) on either side of the equatorial plate are essential for the correct segregation of the chromosomes between the oocyte and polar bodies to ensure genomic integrity. Previous studies have shown that vitrifying–warming GV oocytes reduces the percentage of oocytes with a morphologically normal spindle after IVM compared to their nonvitrified control (52–68% vs 81.3–98.5%). Furthermore, a reduced proportion of vitrified–warmed oocytes exhibited grossly correct chromosome alignment at MII compared with their nonvitrified control (58–68.4% vs 87.5–98.5% respectively; Tharasanit *et al.* 2006; Ortiz-Escribano *et al.* 2018).

It is generally accepted that advanced mare age also has a negative effect on fertility. Mares older than 14–15 years not only show a reduced likelihood of pregnancy at Day 15 after ovulation, but also an increased risk of pregnancy loss (Morris and Allen 2002; Allen *et al.* 2007; Carnevale 2008). Similar to women, it is probable that the increased likelihood of pregnancy loss in aged mares is a factor of aneuploidy arising in the oocyte and/or embryo. We recently demonstrated that *in vitro*-matured oocytes from old mares were more likely to suffer from chromosome misalignment than oocytes from young mares, indicating that advanced maternal age predisposes oocytes to disturbances of spindle function (Rizzo *et al.* 2019). The aim of the present study was to evaluate the effect of vitrifying horse oocytes at the GV stage on subsequent MII spindle architecture and chromosome alignment. We hypothesised that GV oocytes from young mares would be more resistant to any detrimental effects of vitrification than oocytes from old mares, and would therefore show a lower incidence of spindle abnormalities and chromosome misalignment after warming and maturation.

Materials and methods

Collection of GV stage oocytes

Ovaries were collected within 15 min after mares were killed at an abattoir. The ovaries were divided into two groups on the basis of mare age (young ≤14 years; old ≥16 years), as determined from the passport corresponding to the mare's microchip number. Ovaries were transported at 21–25°C to the laboratory within 5 h. Immediately after arrival at the laboratory, cumulus–oocyte complexes (COCs) were harvested by scraping the inner wall of individual follicles with a bone curette and then flushing the scrapings out with 31°C phosphate-buffered saline (PBS; B.Braun) supplemented with 0.5% (v/v) penicillin/streptomycin (GIBCO BRL Life Technologies), as described previously (Hinrichs *et al.* 1993). All visible follicles >3 and ≤30 mm in diameter were selected for scraping to avoid collecting oocytes from follicles too small to be developmentally competent or that had already matured. The COCs in the scrapings were identified using a dissecting stereomicroscope (Leica Wild M3C; Leica Microsystems) equipped with a warming plate set at 37°C and maintained in Euroflush (IMV Technologies) supplemented with 0.4% heparin (5000 IU mL^{-1}; Leo Pharma). Within each age category, COCs were then randomly subdivided into two groups. Oocytes in the control group were matured *in vitro* for 26 h. Oocytes in the vitrification group were first subjected to cumulus 'debulking' (i.e. gentle pipetting to remove outer cumulus cells; Ortiz-Escribano *et al.* 2018) until only the innermost corona radiata layer remained and were then vitrified, as described below. Vitrified oocytes were stored in liquid nitrogen (LN_2) until warming. After warming, the oocytes were matured *in vitro* identically to the control group.

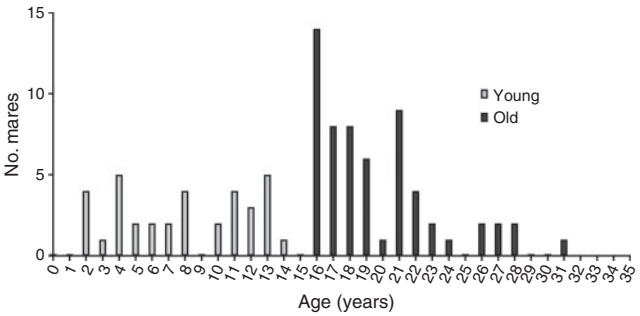

Fig. 1. Overview of the age distribution of young (≤14 years) and old (≥16 years) donor mares.

In all, 605 COCs were recovered from 96 mares (311 COCs from 35 young mares and 294 COCs from 61 old mares). The age of mares in the young group ranged from 2 to 14 years (mean (± s.d.) age 7.9 ± 3.9 years), compared with 16–31 years (mean (± s.d.) 19.6 ± 3.7 years) in the old group (Fig. 1). In all, 319 COCs (169 from young mares, 150 from old mares) were used as controls and matured *in vitro* directly, and 286 COCs (142 from young mares, 144 from old mares) were vitrified and warmed before IVM.

Vitrification and warming

Oocytes were vitrified using the protocol described by Tharasanit *et al.* (2006) with some modifications. Briefly, COCs were incubated for 1 min in a 100-µL droplet of base solution (BS) consisting of TCM-199 Hanks (Gibco) supplemented with 0.014% bovine serum albumin (BSA; Sigma-Aldrich Chemical). Next, COCs were equilibrated for 25 s in a 100-µL droplet of equilibration solution (EqS) consisting of 10% (v/v) ethylene glycol (EG; Sigma-Aldrich) and 10% (v/v) dimethyl sulfoxide (DMSO; Sigma-Aldrich) in BS. Finally, the COCs were transferred to a 100-µL droplet of vitrification solution (VS) consisting of 20% EG, 20% DMSO and 0.5 M sucrose (Sigma-Aldrich) in BS. After 15 s in VS, COCs were transferred to a 1-µL inoculation loop (Soft Loop 1 µL sterile; VWR) as described by Marco-Jiménez *et al.* (2016), plunged immediately

into LN_2 and stored in LN_2 for 1–2 months until warming. The incubations in BS, EqS and VS were performed at 37°C.

Vitrified COCs were subsequently warmed by immersing the inoculation loop in 5 mL warming solution (WS) consisting of BS supplemented with 0.5 M sucrose (Sigma-Aldrich) at 37°C. The COCs were allowed to equilibrate in WS for 5 min before being transferred to BS.

In vitro *maturation*

Groups of four to ten COCs were matured *in vitro* in 500-μL droplets of a 50 : 50 mixture of Dulbecco's modified Eagle's medium (DMEM; Gibco) and Hams F12 (Gibco) supplemented with 10% fetal calf serum (Sigma-Aldrich), 0.125 μg mL^{-1} epidermal growth factor (Peptrotech), 0.1 IU mL^{-1} FSH, 0.6 mM cysteine (Sigma-Aldrich), 0.1 mM cysteamine (Sigma-Aldrich) and 0.1% insulin–transferrin–sodium selenite (Corning Life Science) for 26 h at 38.5°C in a humidified atmosphere of 5% CO_2 in air. The cumulus (if still present) and corona radiata were then removed from the oocytes by incubation in 0.01% hyaluronidase in HEPES-buffered synthetic oviduct fluid (H-SOF; Avantea) and gentle pipetting through 55- and 131-μm plastic pipettes (EZ-strip; Origio). Oocytes were then evaluated using an inverted microscope (Olympus IX71) and scored as mature (MII) if the first polar body was extruded, indicating that the oocyte had completed the first meiotic division. Viable oocytes that did not exhibit a polar body were classified as having failed to complete maturation. Oocytes exhibiting a high degree of cytoplasmic granulation or vacuolation were classified as degenerated. Only oocytes with a visible polar body were fixed, stained and prepared for confocal microscopy.

Fixation and fluorescent labelling of oocytes

Oocyte fixation and fluorescent labelling was performed as described previous by Tharasanit *et al.* (2006), with slight modifications. Briefly, MII oocytes were fixed by first immersing them in microtubule stabilising solution (Medium M; Simerly and Schatten 1993) for 1 h at 38°C, followed by 2% paraformaldehyde for 20 min at room temperature; the oocytes were then stored at 4°C until immunostaining. Prior to staining, oocytes were washed three times in PBS containing 3 mg mL^{-1} polyvinylpyrrolidone (PVP; Sigma-Aldrich) for 5 min before incubation overnight at 4°C in PBS containing a 1 : 250 dilution of a mouse monoclonal anti-α-tubulin antibody (T5168; Sigma-Aldrich) to label the microtubules of the spindle. The oocytes were then washed twice in 0.1% BSA (Sigma-Aldrich) in PBS for 5 min and incubated for 1 h at room temperature in a blocking solution containing 0.1 M glycine, 1% goat serum, 0.01% Triton X-100, 0.5% BSA and 0.02% sodium azide (all from Sigma-Aldrich) in PBS. Thereafter, the oocytes were incubated for 1 h at 37°C in PBS containing 0.5% Triton X-100, 0.5% BSA and 1 : 100 goat anti-mouse Alexa Fluor 488 antibody (A11029; Invitrogen). After two 5-min washing steps in PBS supplemented with 0.1% BSA and 0.1% Triton X-100 and one wash in PBS alone, the oocytes were incubated for 30 min at room temperature in PBS-PVP containing 1 : 100 Hoechst 33342 (Sigma-Aldrich) to label the DNA, and then washed three times in PBS-PVP for 5 min each time. Stained oocytes were mounted on glass microscope slides (SuperfrostPlus; Menzel) in a 10-μL droplet of antifade mounting medium (Vectashield; Vector Laboratories) and sealed under a coverslip using nail polish.

Confocal microscopic imaging and three-dimensional evaluation of spindle morphology and chromosome alignment

The stained oocytes were examined using a Leica TCS-SP5 confocal laser scanning microscope equipped with a ×63 objective. A combination of a 351- and 488-nm laser was used to excite the Hoechst 33342 and Alexa Fluor 488 respectively. The Hoechst 33342 and Alexa Fluor 488 emissions were detected at 414–466 nm (blue channel) and 511–577 nm (green channel), respectively. The meiotic spindle and chromosomes were identified and sequential confocal sections were recorded at 0.42-μm intervals. The images produced by both lasers were then merged using the Leica Application Suite X software. These data were then imported into Imaris 8.2 software (Bitplane) to produce a three-dimensional (3D) image of both the meiotic spindle and chromosomes. The Imaris surface tool was used to render solid surfaces best representing both the spindle and chromosomes, regardless of spindle orientation, as described previously by Rizzo *et al.* (2019). The surface tool of Imaris was used to create a 3D image of the meiotic spindle by selecting the green channel, applying a Gaussian smoothing filter (detail level of 0.0853 μm) and a threshold for absolute intensity that used 51 and 166 arbitrary units as lower and upper thresholds respectively.

The 3D image of the metaphase plate was created in a similar manner by selecting the blue channel and using 27.2 and 213 arbitrary units as the lower and upper thresholds for absolute fluorescence intensity respectively.

Meiotic spindle morphology and chromosome alignment of each MII oocyte were evaluated visually by rotating the 3D image. The spindle was classified as described previously by Rizzo *et al.* (2019). Briefly, a spindle was classified as bipolar when two distinct poles were visible. If three or more poles were observed, or when there was a complete absence of spindle formation, the spindles were classified as severely misshapen and excluded from further measurements (Fig. 2). 3D measurements of the spindle (pole-to-pole length and spindle width) were obtained from the ellipsoid statistics of the Imaris surface tool. Chromosomes were considered to be misaligned when they were displaced by ≥2 μm from the metaphase plate, as described by Coticchio *et al.* (2013). Chromosome misalignment was scored as absent when all the chromosomes were aligned at the metaphase plate, mild when one to five chromosomes were displaced from the metaphase plate and severe when more than five chromosomes were displaced, as described by Rizzo *et al.* (2019; Fig. 2). DNA dispersion was assessed by creating a 3D bounding box (a rectangular prism) around the metaphase plate and measuring the width of this box (the length of the side parallel to the spindle's main axis). Misaligned chromosomes (i.e. chromosomes that were not aligned on the metaphase plate) were excluded from this bounding box.

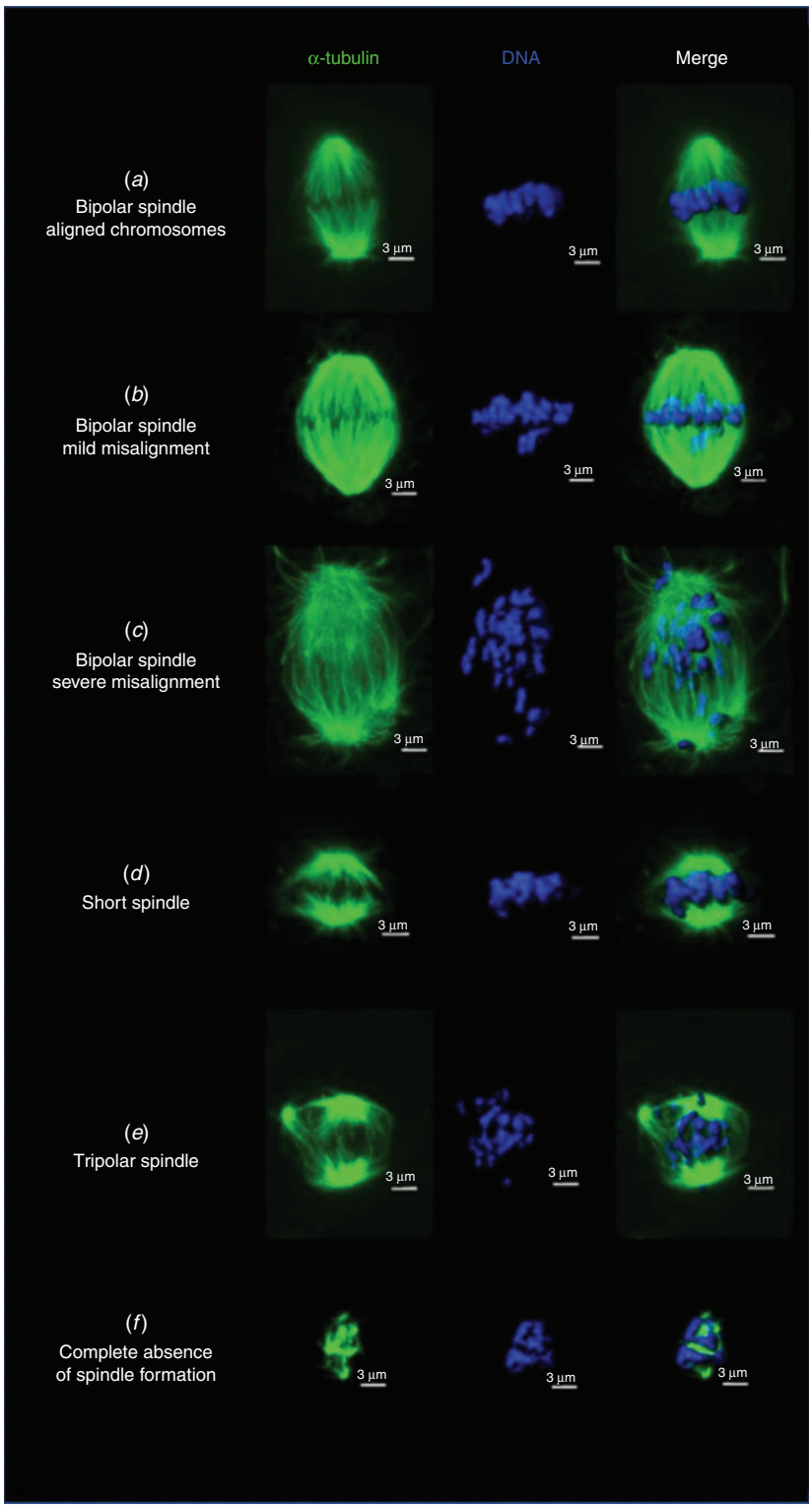

Fig. 2. Confocal micrographs of equine oocytes vitrified at the germinal vesicle stage and subsequently matured *in vitro*. (*a*) A bipolar spindle with chromosomes aligned properly along the metaphase plate. (*b*) A bipolar spindle with mild misalignment of chromosomes (defined as one to five misaligned chromosomes). (*c*) A bipolar spindle with severe misalignment of chromosomes (i.e. more than five misaligned chromosomes). (*d*) A bipolar spindle with reduced pole-to-pole length, but all chromosomes properly aligned along the metaphase plate. (*e*) A tripolar spindle. (*f*) Complete failure of spindle formation.

Data analysis

Data were analysed using the SPSS Statistics 24.0 (IBM). A univariable logistic regression model was used for MII versus non-MII for age and vitrification separately. Subsequently, we used a multivariable model incorporating age, vitrification and their interaction and using a backward

Table 1. Overview of the outcome of IVM for equine oocytes harvested from young (≤14 years) and old (≥16 years) mares and placed immediately into maturation medium (control) or vitrified at the germinal vesicle stage before IVM

Age group	Treatment	No. oocytes	No. degenerated (%)	No. failed to mature (%)	No. MII oocytes (%)
Young	Control	169	79 (47)	15 (9)	75 (44)
	Vitrified	142	76 (53)	28 (20)	38 (27)
Old	Control	150	63 (42)	23 (15)	64 (43)
	Vitrified	144	71 (49)	25 (17)	48 (33)

selection step. The same modelling procedure was used for the outcomes degenerated versus failed to complete maturation, aligned versus misaligned, mild versus severe misalignment and bipolar versus severely misshapen. We used general linear models for spindle length, spindle width and metaphase plate thickness, where age, vitrification and their interaction were included as explanatory variables. We simplified the model using a backwards selection step. A visual inspection of the residuals showed no deviations from the model's assumptions for any parameter.

Results

Oocyte collection and maturation

Vitrification reduced the odds of an oocyte reaching MII regardless of the age of the donor mare (odds ratio (OR) 0.6; 95% confidence interval (CI) 0.4–0.8; Table 1). No significant interaction between age and vitrification was evident. Furthermore, vitrification did not increase the likelihood of oocytes degenerating or failing to mature, regardless of donor mare age.

Spindle morphology

Seventeen vitrified–warmed MII oocytes from young mares and eight from old mares were excluded due to inadequate chromatin staining ($n = 5$ young and 2 old) or because they were lost during processing ($n = 12$ young and 6 old). In the control group, two young mare and five old mare oocytes were excluded due to inadequate chromatin staining. Therefore, a total of 60 vitrified–warmed (21 from young mares, 39 from old mares) and 53 control (23 from young mares, 30 from old mares) oocytes were eventually evaluated.

The odds of spindle abnormalities increased after vitrification of oocytes from both young (OR 6.0; 95% CI 2.9–9.1) and old (OR 1.3; 95% CI 1.3–27.5) mares (Fig. 3). The spindle major axis (i.e. spindle length) of oocytes originating from young mares that were vitrified was, on average, 8.9 μm shorter than that of non-vitrified controls (95% CI −12.3, −5.6). The spindle major axis of oocytes originating from old mares was, on average, 1.99 μm shorter after vitrification, but this difference was not statistically significant (95% CI −4.6, 0.6; Fig. 4). Conversely, the spindle minor axis (i.e. spindle width) was, on average, 1.5 μm shorter in vitrified than control oocytes (95% CI −2.3, −0.6), regardless of the age of mares or of any interaction between age and vitrification (Fig. 5).

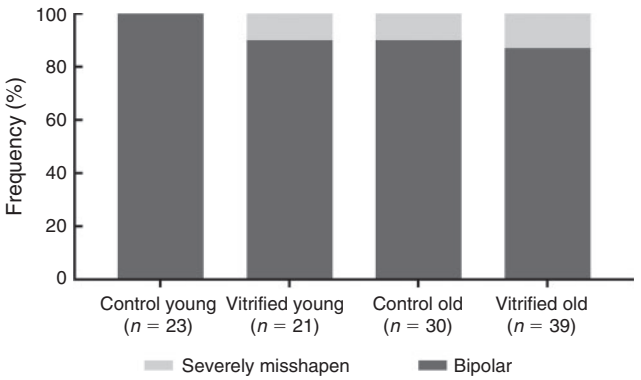

Fig. 3. Incidence of bipolar versus severely misshapen MII spindles (i.e. tri- or tetrapolar or the complete absence of spindle formation) in vitrified–warmed and control equine oocytes from young (≤14 years) and old (≥16 years) donor mares.

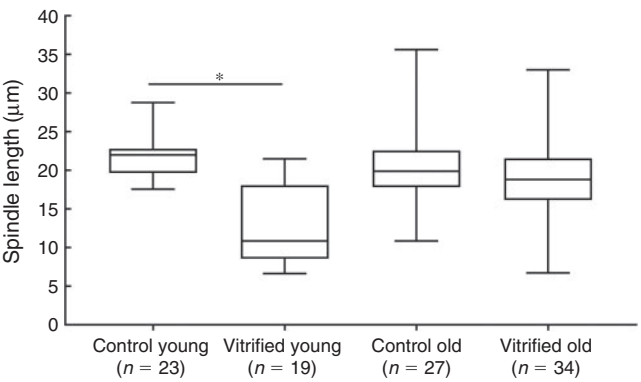

Fig. 4. Box plot showing spindle length (pole-to-pole) in vitrified–warmed and control oocytes from young (≤14 years) and old (≥16 years) donor mares following maturation *in vitro*. The boxes show the interquartile range, with the median value indicated by the horizontal line; whiskers show the range. *$P < 0.05$.

Chromosome alignment and DNA dispersion

Within oocytes originating from young mares, vitrification resulted in significantly higher odds of chromosome misalignment (OR 78.3; 95% CI 4.12–1486). This was not the case for oocytes originating from old donor mares (OR 1.4; 95% CI 0.5–3.9). However, within the old mare oocytes exhibiting

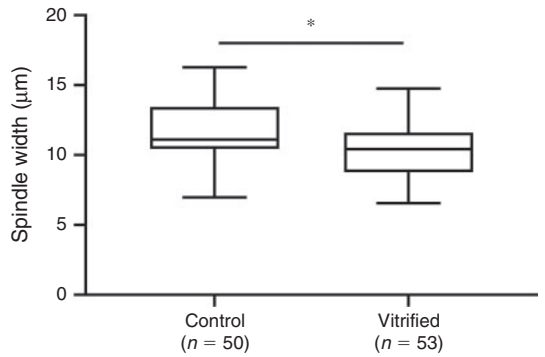

Fig. 5. Box plot showing spindle width in vitrified–warmed and control oocytes following maturation *in vitro*. The boxes show the interquartile range, with the median value indicated by the horizontal line; whiskers show the range. $*P < 0.05$.

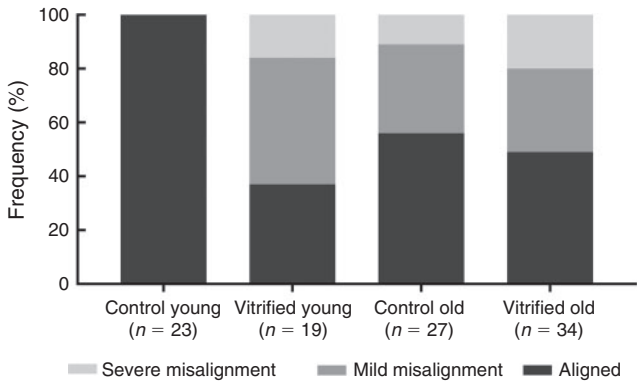

Fig. 6. Frequency of chromosome misalignment in MII oocytes from vitrified–warmed and control equine oocytes originating from young (≤14 years) and old (≥16 years) mares following maturation *in vitro*. Aligned, all chromosomes were aligned on the metaphase plate; mild, one to five misaligned chromosomes; severe, more than five misaligned chromosomes.

misalignment, the odds of severe misalignment (defined as the presence of more than five misaligned chromosomes on the metaphase spindle) was significantly higher after vitrification (OR 1.9; 95% CI 0.38–9.59; Fig. 6).

The metaphase plate thickness of vitrified oocytes originating from young mares was, on average, 1.3 μm thicker than that of non-vitrified control oocytes (95% CI 0.5–2.1). In oocytes originating from old mares, there was an average increase in metaphase plate thickness of 0.04 μm after vitrification, but this was not statistically significant (95% CI −0.6, 0.7; Fig. 7).

Discussion

The DNA within GV oocytes is condensed, but not yet organised into chromosomes, and protected by a nuclear membrane. At the GV stage, the spindle apparatus, which organises chromosome alignment and subsequent segregation to ensure formation of a euploid gamete, has yet to form. This configuration reduces, at least in theory, the risk of chromosome segregation errors and aneuploidy after cryopreservation compared with MII oocytes.

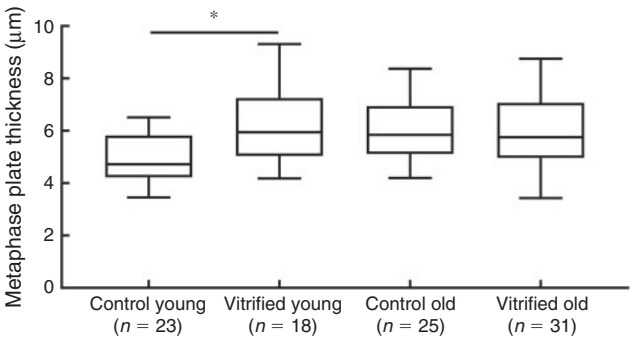

Fig. 7. Metaphase plate thickness in vitrified–warmed and control oocytes from young (≤14 years) and old (≥16 years) donor mares following maturation *in vitro*. The boxes show the interquartile range, with the median value indicated by the horizontal line; whiskers show the range. $*P < 0.05$.

In MII oocytes, the DNA is condensed into chromosomes that are aligned at the equator of a highly specialised cytoplasmic structure, the spindle. The tubulin filaments that form the spindle are highly susceptible to cryodamage capable of inducing microtubule depolymerisation, disorganisation and aneuploidy (Tharasanit *et al.* 2006). Conversely, vitrified–warmed GV stage oocytes need to successfully assemble a spindle and complete nuclear maturation, accompanied by adequate cytoplasmic maturation, if they are to maintain their developmental competence. Despite the theoretically 'less susceptible to cryodamage' configuration of GV than MII oocytes, vitrification is still associated with poor embryo development in various species, including humans (Park *et al.* 1997), mice (Cheng *et al.* 2014), pigs (Rojas *et al.* 2004), cows (Magnusson *et al.* 2008) and horses (Tharasanit *et al.* 2006; Canesin *et al.* 2017, 2018; Ortiz-Escribano *et al.* 2018).

In the present study, we demonstrated that vitrifying–warming equine GV oocytes not only reduced their ability to complete nuclear maturation, as reported previously (Tharasanit *et al.* 2006; Canesin *et al.* 2017; Ortiz-Escribano *et al.* 2018), but that it also resulted in reductions in spindle length and width accompanied by an increased incidence of chromosome misalignment and DNA dispersion from the metaphase plate. Interestingly, for all features investigated, oocytes from young mares were more affected by vitrification than oocytes from older mares. This was contrary to our expectation that oocytes from old mares would suffer more damage during vitrification. In this regard, we previously reported that MII oocytes from aged mares have an impaired ability to align their chromosomes on the metaphase spindle (Rizzo *et al.* 2019), probably due to a reduced stringency of the spindle assembly checkpoint (SAC) apparatus (Rizzo *et al.* 2016). During cell division, the SAC prevents separation of the duplicated chromosomes until all the chromosomes are properly attached to the spindle apparatus and aligned at the midpoint. The SAC is able to detect unattached microtubules or loss of tension, and impose metaphase arrest until all the chromosomes are correctly aligned at the metaphase plate. Once the chromosomes are properly aligned, the SAC is silenced and cell division is allowed to progress to anaphase. It is possible that the higher sensitivity of oocytes from young mares

to vitrification-induced disturbance is a factor of more complete SAC component expression before vitrification, rendering it more prone to additional damage. Loss of cohesion between duplicated chromatids (Lister *et al.* 2010; Jessberger 2012; Tsutsumi *et al.* 2014), together with impaired SAC function (Vogt *et al.* 2008; Shomper *et al.* 2014), is considered to be the main cause of the increased incidence of aneuploidy in oocytes from both older women and older mice. In the present study, we similarly observed a significantly higher incidence of chromosome misalignment in oocytes from aged compared with younger mares in the non-vitrified group. This may explain the absence of a significant effect of vitrification on the incidence of chromosome misalignment in oocytes from old mares, because the oocytes were already compromised before vitrification.

Not only did we see a decrease in the percentage of oocytes with a bipolar spindle after vitrification–warming, but we also noted a reduction in spindle length. This has been reported previously after vitrification of equine (Tharasanit *et al.* 2006; Maclellan *et al.* 2018; Ortiz-Escribano *et al.* 2018) and feline (Comizzoli *et al.* 2004) GV oocytes. Interestingly, in the present study, spindle length was reduced significantly only after vitrification of young mare oocytes. Although Maclellan *et al.* (2018) used mares of a similar age to our young group (i.e. between 3 and 16 years old), the spindle length measured by Maclellan *et al.* (2018) was longer than that recorded in the present study (mean ($\pm$ s.e.) 16.72 ± 0.41 vs 12.6 ± 1.1 μm respectively). This may be a consequence of the different methods used to measure meiotic spindle length. We used 3D software to allow accurate measurement of the dimensions of the spindle regardless of its orientation during confocal imaging. Moreover, differences in the vitrification protocols used may have contributed to differences in spindle length between the studies. Spindle length is determined by a balance between several cytoplasmic components, including microtubule polymerisation and depolymerisation factors, as well as microtubule-severing proteins (Wang *et al.* 2016). In human oocytes, spindle length is an indicator of oocyte quality; spindles longer than 120 μm and shorter than 90 μm are associated with a lower likelihood of fertilisation, blastocyst formation and clinical pregnancy (Tomari *et al.* 2018). Moreover, it is well known that chromosome misalignment can affect spindle morphology. In fact, when proteins required for the centromere–kinetochore complex are knocked down, both the incidence of chromosome misalignment and spindle length increased in mouse oocytes (Ma *et al.* 2014). Recently, we showed that in horse oocytes spindles containing misaligned chromosomes are longer than spindles with no misaligned chromosomes (Rizzo *et al.* 2019). It is known that cryopreservation can lead to protein damage and changes in protein synthesis (Succu *et al.* 2007, 2008; Wen *et al.* 2007; Wang *et al.* 2017). Vitrification could induce an imbalance in the proteins determining spindle length; this could explain the observed shortening in spindle length after vitrification, but cannot explain why oocytes from young mares are affected but oocytes from old mares are not. Further research is needed to determine whether proteins involved in regulating microtubule formation and breakdown are altered by vitrification. Microtubule polymerisation and spindle formation are also dependent on functional mitochondria (Eichenlaub-Ritter *et al.* 2004) and they may be compromised by vitrification because swelling of mitochondria has been demonstrated after vitrification of equine oocytes (Hochi *et al.* 1996). Thus, impaired mitochondrial function could contribute to alterations in meiotic spindle formation after vitrification. Rambags *et al.* (2014) showed that advanced maternal age is also associated with swelling and loss of cristae in mitochondria after IVM of equine oocytes. Based on this, one would expect oocytes originating from young mares to be less affected by vitrification than oocytes from older mares, but this is contrary to our results. In any case, it is probable that, as in women, mare oocytes with either an abnormally short or an abnormally long spindle are associated with a poor outcome.

In conclusion, vitrifying equine oocytes at the GV stage not only impairs their ability to reach MII during IVM, but also induces ultrastructural changes in the meiotic spindle and impairs their ability to correctly align the chromosomes along the metaphase plate. This is likely to interfere with normal chromosome segregation and thereby predispose to aneuploidy. We propose that these changes to spindle morphology and function may be important contributors to the reduced developmental competence of vitrified–warmed equine GV oocytes. Oocytes from young mares seem to be more affected then oocytes from older mares, which may primarily reflect pre-existing compromise of SAC control mechanisms in the latter.

Conflicts of interest

The authors declare no conflicts of interest.

Acknowledgements

Confocal microscopic images were acquired and 3D analysis was performed at the Centre for Cell Imaging (CCI) at the Faculty of Veterinary Medicine, Utrecht University (Utrecht, Netherlands). The authors thank Richard Wubbolts and Esther van't Veld for their help and technical assistance. The authors also thank Hans Vernooij for his advice on statistical analysis. K. D. Ducheyne's salary was provided by the Agentschap voor Innovatie door Wetenschap en Technologie (IWT; Grant 141492).

References

Allen, W. R., Brown, L., Wright, M., and Wilsher, S. (2007). Reproductive efficiency of Flatrace and National Hunt Thoroughbred mares and stallions in England. *Equine Vet. J.* **39**, 438–445. doi:10.2746/042516407X1737581

Canesin, H. S., Brom-de-Luna, J. G., Choi, Y. H., Ortiz, I., Diaw, M., and Hinrichs, K. (2017). Blastocyst development after intracytoplasmic sperm injection of equine oocytes vitrified at the germinal-vesicle stage. *Cryobiology* **75**, 52–59. doi:10.1016/J.CRYOBIOL.2017.02.004

Canesin, H. S., Brom-de-Luna, J. G., Choi, Y. H., Pereira, A. M., Macedo, G. G., and Hinrichs, K. (2018). Vitrification of germinal-vesicle stage equine oocytes: effect of cryoprotectant exposure time on *in-vitro* embryo production. *Cryobiology* **81**, 185–191. doi:10.1016/J.CRYOBIOL.2018.01.001

Carnevale, E. M. (2008). The mare model for follicular maturation and reproductive aging in the woman. *Theriogenology* **69**, 23–30. doi:10.1016/J.THERIOGENOLOGY.2007.09.011

Cheng, J., Jia, B., Wu, T., Zhou, G., Hou, Y., Fu, X., and Zhu, S. (2014). Effects of vitrification for germinal vesicle and metaphase II oocytes on subsequent centromere cohesion and chromosome aneuploidy in mice. *Theriogenology* **82**, 495–500. doi:10.1016/J.THERIOGENOLOGY.2014.05.009

Choi, Y. H., Love, L. B., Varner, D. D., and Hinrichs, K. (2006). Holding immature equine oocytes in the absence of meiotic inhibitors: effect on germinal vesicle chromatin and blastocyst development after intracytoplasmic sperm injection. *Theriogenology* **66**, 955–963. doi:10.1016/J.THERIOGENOLOGY.2006.01.064

Choi, Y. H., Velez, I. C., Macias-Garcia, B., Riera, F. L., Ballard, C. S., and Hinrichs, K. (2016). Effect of clinically-related factors on *in vitro* blastocyst development after equine ICSI. *Theriogenology* **85**, 1289–1296. doi:10.1016/J.THERIOGENOLOGY.2015.12.015

Comizzoli, P., Wildt, D. E., and Pukazhenthi, B. S. (2004). Effect of 1,2-propanediol versus 1,2-ethanediol on subsequent oocyte maturation, spindle integrity, fertilization, and embryo development *in vitro* in the domestic cat. *Biol. Reprod.* **71**, 598–604. doi:10.1095/BIOLREPROD.104.027920

Coticchio, G., Guglielmo, M. C., Dal Canto, M., Fadini, R., Mignini Renzini, M., De Ponti, E., Brambillasca, F., and Albertini, D. F. (2013). Mechanistic foundations of the metaphase II spindle of human oocytes matured *in vivo* and *in vitro*. *Hum. Reprod.* **28**, 3271–3282. doi:10.1093/HUMREP/DET381

Curcio, B. R., Gastal, M. A., Pereira, G. R., Corcini, C. D., Landim-Alvarenga, F. C., Barros, S. S., Nogueira, C. E. W., Deschamps, J. C., and Gastal, E. L. (2014). Ultrastructural morphology and nuclear maturation rates of immature equine oocytes vitrified with different solutions and exposure times. *J. Equine Vet. Sci.* **34**, 632–640. doi:10.1016/J.JEVS.2013.12.002

de Leon, P. M., Campos, V. F., Corcini, C. D., Santos, E. C., Rambo, G., Lucia, T. Jr, Deschamps, J. C., and Collares, T. (2012). Cryopreservation of immature equine oocytes, comparing a solid surface vitrification process with open pulled straws and the use of a synthetic ice blocker. *Theriogenology* **77**, 21–27. doi:10.1016/J.THERIOGENOLOGY.2011.07.008

Eichenlaub-Ritter, U., Vogt, E., Yin, H., and Gosden, R. (2004). Spindles, mitochondria and redox potential in ageing oocytes. *Reprod. Biomed. Online* **8**, 45–58. doi:10.1016/S1472-6483(10)60497-X

Galli, C., Colleoni, S., Duchi, R., Lagutina, I., and Lazzari, G. (2007). Developmental competence of equine oocytes and embryos obtained by *in vitro* procedures ranging from *in vitro* maturation and ICSI to embryo culture, cryopreservation and somatic cell nuclear transfer. *Anim. Reprod. Sci.* **98**, 39–55. doi:10.1016/J.ANIREPROSCI.2006.10.011

Galli, C., Colleoni, S., Turini, P., Crotti, G., Dieci, C., Lodde, V., Luciano, A. M., and Lazzari, G. (2014). Holding equine oocytes at room temperature for 18 hours prior *in vitro* maturation maintains their developmental competence. *J. Equine Vet. Sci.* **34**, 174–175. doi:10.1016/J.JEVS.2013.10.128

Hinrichs, K., Schmidt, A. L., Friedman, P. P., Selgrath, J. P., and Martin, M. G. (1993). *In vitro* maturation of horse oocytes: characterization of chromatin configuration using fluorescence microscopy. *Biol. Reprod.* **48**, 363–370. doi:10.1095/BIOLREPROD48.2.363

Hochi, S., Kozawa, M., Fujimoto, T., Hondo, E., Yamada, J., and Oguri, N. (1996). *In vitro* maturation and transmission electron microscopic observation of horse oocytes after vitrification. *Cryobiology* **33**, 300–310. doi:10.1006/CRYO.1996.0030

Hurtt, A. E., Landim-Alvarenga, F., Seidel, G. E., Jr, and Squires, E. L. (2000). Vitrification of immature and mature equine and bovine oocytes in an ethylene glycol, ficoll and sucrose solution using open-pulled straws. *Theriogenology* **54**, 119–128. doi:10.1016/S0093-691X(00)00330-7

Jessberger, R. (2012). Age-related aneuploidy through cohesion exhaustion. *EMBO Rep.* **13**, 539–546. doi:10.1038/EMBOR.2012.54

Lister, L. M., Kouznetsova, A., Hyslop, L. A., Kalleas, D., Pace, S. L., Barel, J. C., Nathan, A., Floros, V., Adelfalk, C., Watanabe, Y., Jessberger, R., Kirkwood, T. B., Hoog, C., and Herbert, M. (2010). Age-related meiotic segregation errors in mammalian oocytes are preceded by depletion of cohesin and Sgo2. *Curr. Biol.* **20**, 1511–1521. doi:10.1016/J.CUB.2010.08.023

Ma, R., Hou, X., Zhang, L., Sun, S. C., Schedl, T., Moley, K., and Wang, Q. (2014). Rab5a is required for spindle length control and kinetochore–microtubule attachment during meiosis in oocytes. *FASEB J.* **28**, 4026–4035. doi:10.1096/FJ.14-250886

Maclellan, L. J., Hatzel, J. N., Amoroso, F., Stokes, J. E., and Carnevale, E. M. (2018). Meiotic spindle characteristics of oocytes after vitrification at germinal vesicle stage, warming and maturation *in vitro* and developmental potential after ICSI. *J. Equine Vet. Sci.* **66**, 202. doi:10.1016/J.JEVS.2018.05.091

Magnusson, V., Feitosa, W. B., Goissis, M. D., Yamada, C., Tavares, L. M., D'Avila Assumpcao, M. E., and Visintin, J. A. (2008). Bovine oocyte vitrification: effect of ethylene glycol concentrations and meiotic stages. *Anim. Reprod. Sci.* **106**, 265–273. doi:10.1016/J.ANIREPROSCI.2007.05.001

Marco-Jiménez, F., Jiménez-Trigos, E., Almela-Miralles, V., and Vicente, J. S. (2016). Development of cheaper embryo vitrification device using the minimum volume method. *PLoS One* **11**, e0148661. doi:10.1371/JOURNAL.PONE.0148661

Morris, L. H., and Allen, W. R. (2002). Reproductive efficiency of intensively managed Thoroughbred mares in Newmarket. *Equine Vet. J.* **34**, 51–60. doi:10.2746/042516402776181222

Ortiz-Escribano, N., Bogado Pascottini, O., Woelders, H., Vandenberghe, L., De Schauwer, C., Govaere, J., Van den Abbeel, E., Vullers, T., Ververs, C., Roels, K., Van De Velde, M., Van Soom, A., and Smits, K. (2018). An improved vitrification protocol for equine immature oocytes, resulting in a first live foal. *Equine Vet. J.* **50**, 391–397. doi:10.1111/EVJ.12747

Park, S. E., Son, W. Y., Lee, S. H., Lee, K. A., Ko, J. J., and Cha, K. Y. (1997). Chromosome and spindle configurations of human oocytes matured *in vitro* after cryopreservation at the germinal vesicle stage. *Fertil. Steril.* **68**, 920–926. doi:10.1016/S0015-0282(97)00365-8

Rader, K., Choi, Y. H., and Hinrichs, K. (2016). Intracytoplasmic sperm injection, embryo culture, and transfer of *in vitro*-produced blastocysts. *Vet. Clin. North Am. Equine Pract.* **32**, 401–413. doi:10.1016/J.CVEQ.2016.07.003

Rambags, B. P., van Boxtel, D. C., Tharasanit, T., Lenstra, J. A., Colenbrander, B., and Stout, T. A. (2014). Advancing maternal age predisposes to mitochondrial damage and loss during maturation of equine oocytes *in vitro*. *Theriogenology* **81**, 959–965. doi:10.1016/J.THERIOGENOLOGY.2014.01.020

Rizzo, M., de Ruijter-Villani, M., Deelen, C., Beitsma, M., Cristarella, S., Quartuccio, M., and Stout, T. A. E. (2016). Oocytes from aged mares show reduced expression of mRNA for key spindle assembly checkpoint components. *J. Equine Vet. Sci.* **41**, 84. doi:10.1016/J.JEVS.2016.04.088

Rizzo, M., Ducheyne, K. D., Deelen, C., Beitsma, M., Cristarella, S., Quartuccio, M., Stout, T. A. E., and de Ruijter-Villani, M. (2019). Advanced mare age impairs the ability of *in vitro*-matured oocytes to correctly align chromosomes on the metaphase plate. *Equine Vet. J.* **51**, 252–257. doi:10.1111/EVJ.12995

Rojas, C., Palomo, M. J., Albarracin, J. L., and Mogas, T. (2004). Vitrification of immature and *in vitro* matured pig oocytes: study of distribution of chromosomes, microtubules, and actin microfilaments. *Cryobiology* **49**, 211–220. doi:10.1016/J.CRYOBIOL.2004.07.002

Roser, J. F., and Meyers-Brown, G. (2012). Superovulation in the mare: a work in progress. *J. Equine Vet. Sci.* **32**, 376–386. doi:10.1016/J.JEVS.2012.05.055

Shomper, M., Lappa, C., and FitzHarris, G. (2014). Kinetochore microtubule establishment is defective in oocytes from aged mice. *Cell Cycle* **13**, 1171–1179. doi:10.4161/CC.28046

Simerly, C., and Schatten, G. (1993). Techniques for localization of specific molecules in oocytes and embryos. *Methods Enzymol.* **225**, 516–553. doi:10.1016/0076-6879(93)25035-Z

Succu, S., Leoni, G. G., Bebbere, D., Berlinguer, F., Mossa, F., Bogliolo, L., Madeddu, M., Ledda, S., and Naitana, S. (2007). Vitrification devices affect structural and molecular status of *in vitro* matured ovine oocytes. *Mol. Reprod. Dev.* **74**, 1337–1344. doi:10.1002/MRD.20693

Succu, S., Bebbere, D., Bogliolo, L., Ariu, F., Fois, S., Leoni, G. G., Berlinguer, F., Naitana, S., and Ledda, S. (2008). Vitrification of *in vitro* matured ovine oocytes affects *in vitro* pre-implantation development and mRNA abundance. *Mol. Reprod. Dev.* **75**, 538–546. doi:10.1002/MRD.20784

Tharasanit, T., Colleoni, S., Lazzari, G., Colenbrander, B., Galli, C., and Stout, T. A. (2006). Effect of cumulus morphology and maturation stage on the cryopreservability of equine oocytes. *Reproduction* **132**, 759–769. doi:10.1530/REP.1.01156

Tomari, H., Honjo, K., Kunitake, K., Aramaki, N., Kuhara, S., Hidaka, N., Nishimura, K., Nagata, Y., and Horiuchi, T. (2018). Meiotic spindle size is a strong indicator of human oocyte quality. *Reprod. Med. Biol.* **17**, 268–274. doi:10.1002/RMB2.12100

Tsutsumi, M., Fujiwara, R., Nishizawa, H., Ito, M., Kogo, H., Inagaki, H., Ohye, T., Kato, T., Fujii, T., and Kurahashi, H. (2014). Age-related decrease of meiotic cohesins in human oocytes. *PLoS One* **9**, e96710. doi:10.1371/JOURNAL.PONE.0096710

Vogt, E., Kirsch-Volders, M., Parry, J., and Eichenlaub-Ritter, U. (2008). Spindle formation, chromosome segregation and the spindle checkpoint in mammalian oocytes and susceptibility to meiotic error. *Mutat. Res.* **651**, 14–29. doi:10.1016/J.MRGENTOX.2007.10.015

Wang, Z. W., Zhang, G. L., Schatten, H., Carroll, J., and Sun, Q. Y. (2016). Cytoplasmic determination of meiotic spindle size revealed by a unique inter-species germinal vesicle transfer model. *Sci. Rep.* **6**, 19827. doi:10.1038/SREP19827

Wang, N., Li, C. Y., Zhu, H. B., Hao, H. S., Wang, H. Y., Yan, C. L., Zhao, S. J., Du, W. H., Wang, D., Liu, Y., Pang, Y. W., and Zhao, X. M. (2017). Effect of vitrification on the mRNA transcriptome of bovine oocytes. *Reprod. Domest. Anim.* **52**, 531–541. doi:10.1111/RDA.12942

Wen, Y., Quintero, R., Chen, B., Shu, Y., Polan, M. L., and Behr, B. (2007). Expression of CD9 in frozen–thawed mouse oocytes: preliminary experience. *Fertil. Steril.* **88**, 526–529. doi:10.1016/J.FERTNSTERT.2006.11.130